

**Non-Gaussian resistance noise in the ferromagnetic insulating state of a hole-doped manganite**

Sudeshna Samanta\* and A. K. Raychaudhuri†

*Department of Materials Science, S. N. Bose National Centre for Basic Sciences, Block JD, Sector 3, Salt Lake, Kolkata 700 098, West Bengal, India*

Ya. M. Mukhovskii

*National University of Science and Technology MISIS, Leninsky Pros. 4, Moscow 119049, Russian Federation*

(Received 20 August 2011; revised manuscript received 2 December 2011; published 25 January 2012)

We report the observation of a large  $1/f$  noise in the ferromagnetic insulating state (FMI) of a hole doped manganite single crystal of  $\text{La}_{0.80}\text{Ca}_{0.20}\text{MnO}_3$ , which manifests hopping conductivity in the presence of a Coulomb gap. The temperature-dependent noise magnitude decreases in the FMI state indicating a sharp freeze-out of the noise magnitude with temperature on cooling. As the material is cooled down below the ferromagnetic transition  $T_C$ , the noise becomes non-Gaussian, as seen through the probability density function and second spectra. On further cooling in the FMI state, the noise becomes more non-Gaussian. The non-Gaussian noise is proposed to arise from charge fluctuations in a correlated glassy phase of the polaronic carriers which develop in these systems, as reported in recent simulation studies.

DOI: [10.1103/PhysRevB.85.045127](https://doi.org/10.1103/PhysRevB.85.045127)

PACS number(s): 71.27.+a, 71.30.+h, 72.70.+m

**I. INTRODUCTION**

Electronic transport through localized states in disordered and correlated electronic systems has been a topic of considerable interest.<sup>1-3</sup> A fascinating state appears at a low hole doping level, where the ground state of the system has become ferromagnetic but not yet metallic. The unexpected coexistence of ferromagnetism and insulating behavior seems to contradict the conventional double exchange<sup>4</sup> model. The origin of this coexistence is not clear but might stem from a delicate balance of charge localization by orbital ordering (OO),<sup>5</sup> due to the Jahn Teller effect, and ferromagnetic interactions between  $\text{Mn}^{3+}$  and  $\text{Mn}^{4+}$  ions.<sup>6</sup> Some theoretical<sup>7</sup> and experimental<sup>8</sup> results suggest that the OO is an important factor for controlling the electron-hole mobility. In such systems, long-range Coulomb interaction can lead to opening up of a soft gap in the density of states (referred to as the Coulomb gap,  $\Delta_{\text{CG}}$ ) and hopping conduction in the presence of such a gap.<sup>9</sup> Another consequence is the emergence of “glassy” slow relaxations of charge carriers arising from a large number of low-lying states separated by barriers.<sup>10</sup> Such a glassy phase can lead to enhanced low-frequency ( $f$ ) non-Gaussian resistance noise (typically with a power spectrum varying as  $1/f$ )<sup>11,12</sup> arising from charge fluctuations.<sup>13,14</sup> These issues in a Coulomb glass have been reviewed recently.<sup>2</sup> The experimental investigations on these questions are few and were carried out only in the doped semiconductors with electron density close to the critical concentration ( $n_C$ ) for the metal-insulator (MI) transition<sup>15,16</sup> or in two-dimensional electron glass in MOSFET's.<sup>17</sup> Here, we focus on the issue of non-Gaussian low-frequency noise in the Coulomb glass phase of a very different material, namely, the low hole doped rare-earth manganites which can have a ferromagnetic insulating (FMI) state below a certain temperature ( $T$ ). In these systems, the Coulomb glass phase occurs for the localized polaronic carriers (in sharp contrast to doped semiconductors) which arise due to strong electron-phonon coupling from Jahn-Teller distortion around the  $\text{Mn}^{3+}$  ions.

The FMI state of hole doped manganites ( $\text{La}_{1-x}\text{Ca}_x\text{MnO}_3$ ) arises when hole concentration  $x$  in  $\text{LaMnO}_3$  exceeds the critical concentration for ferromagnetism  $x \approx 0.125$  yet it is smaller than the concentration needed for the formation of the metallic ground state  $x \geq x_C = 0.225$ . This region of the manganite phase diagram is a topic of current investigations<sup>18</sup> and is marked by the presence of a mixed phase of different orbital orders/disorders that can have different conductivities.<sup>5,8,19</sup> In this range of hole doping in manganites at low temperatures, there is a majority insulating ferromagnetic phase that coexists with a conducting phase. The extent of the phase separation of the two phases, the nature of orbital order, will determine the exact physical property, among other things, which can lead to a spin-cluster glass-type behavior arising from competing spin interactions in the presence of disorder. The existence of the glassy behavior with a long-time tail has been seen in time-dependent resistance relaxation<sup>20,21</sup> and also in NMR relaxation studies at low temperatures deep into the FMI state.<sup>6</sup>

In this paper we address the issue of Coulomb interaction and investigate experimentally whether there is a signature of entry into a Coulomb glass phase which can occur along with the spin-cluster glass phase. Existence of a Coulomb glass behavior in the FMI state has been inferred from certain transport experiments<sup>22,23</sup> and also predicted theoretically recently.<sup>24</sup> We observe large low-frequency resistance fluctuations (noise) with nontrivial temperature dependence in the FMI state. As the material is cooled down below the ferromagnetic transition temperature  $T_C$ , the noise becomes non-Gaussian. On further cooling, the noise becomes strongly non-Gaussian. At low temperatures, well below the transition to the insulating state, the noise shows a sharp fall on cooling. We propose below that the large noise as well as its temperature dependence arise from charge fluctuations due to the special nature of carriers in it.

**II. EXPERIMENTAL DETAILS**

We have investigated the low-frequency resistance noise ( $50 \text{ mHz} < f < 10 \text{ Hz}$ ) in a single crystal of the manganite,

$\text{La}_{0.80}\text{Ca}_{0.20}\text{MnO}_3$  (LCMO20). The noise experiments on single crystals allow us to avoid extraneous influences coming from structural defects<sup>25</sup> which may mask the noise arising from some of the intrinsic effects like the one being investigated here.

The crystals used in this work were grown by the floating-zone technique.<sup>26</sup> We note that the exact composition of the crystal was checked by a number of procedures, including a quantitative chemical method like inductively coupled plasma (ICP): atomic emission spectroscopy. The sample chemical inhomogeneity was tested by a microprobe, and the sample used in the experiment was cut from a portion which shows a homogeneous chemical composition over the length and cross section. In addition, we did titration to check the oxygen stoichiometry.

The resistivity ( $\rho$ ) versus  $T$  was measured by four probes (with evaporated contact pads) using the ac biasing technique with phase-sensitive detection procedure. Typical current ( $I$ ) bias was  $\leq 1 \mu\text{A}$ . At low  $T$ , the measured resistance is a strong function of  $I$  when the bias crosses a threshold. As a result, a low-current bias is used.

The noise measurements were carried out with a five-probe<sup>27</sup> ac detection scheme with low ac current,  $I = 1 \mu\text{A}$ . The same contact pads were used for both the resistivity and noise measurements. We use an ac Wheatstone bridge configuration to measure resistance fluctuations, as depicted schematically in Fig. 1(a). Two parts of the sample (with five probes) show that resistances ( $r_1$  and  $r_2$ ) with respect to the ground lead (center port) and serve as two lower arms of the bridge circuit. The resistance of the balancing arms ( $R_1$  and  $R_2$ ) of the bridge are kept much greater than  $r_1$  and  $r_2$  to keep the biasing  $I$  constant. The five-probe ac technique has distinct advantages compared to dc biasing techniques.<sup>28</sup> First, the background noise can be measured simultaneously along with the sample noise which allows the background subtraction more reliable one. Also the noise can be measured with much less measuring power, allowing the measurements to stay close to the equilibrium noise. The background noise was measured at each  $T$  simultaneously and was found to be “white.” The measured noise power for the background noise was found to be very close to the Nyquist value  $4k_B T R$ . This ensures that there is no spurious noise in the measurement system. This also removes the possibility of a changing noise contribution due to a current shunting effect, if any. We have also changed the contact size and relative spacing to ensure that such effects like contacts or current shunting do not affect the measurements.

The details of the method and its practical realization have been discussed previously.<sup>28,29</sup> The output from the amplifier [see Fig. 1(a)] was digitized as a time series. A typical example is shown in the inset of Figs. 1(b) and 1(c). The technique uses a sample bias with carrier frequency  $f_c$  (we used typically  $f_c = 228 \text{ Hz}$ ) which is chosen to be the frequency region where detection of electronics noise is low. This minimizes considerably the  $1/f$  noise of the detection electronics, which is a problem for dc noise measurements. The voltage fluctuation arises as a side band of  $f_c$  after demodulation of the  $f_c$  by the lock-in amplifier (LIA). The demodulated signal is fed to the differential input of the analog-to-digital converter (ADC) card. The demodulated

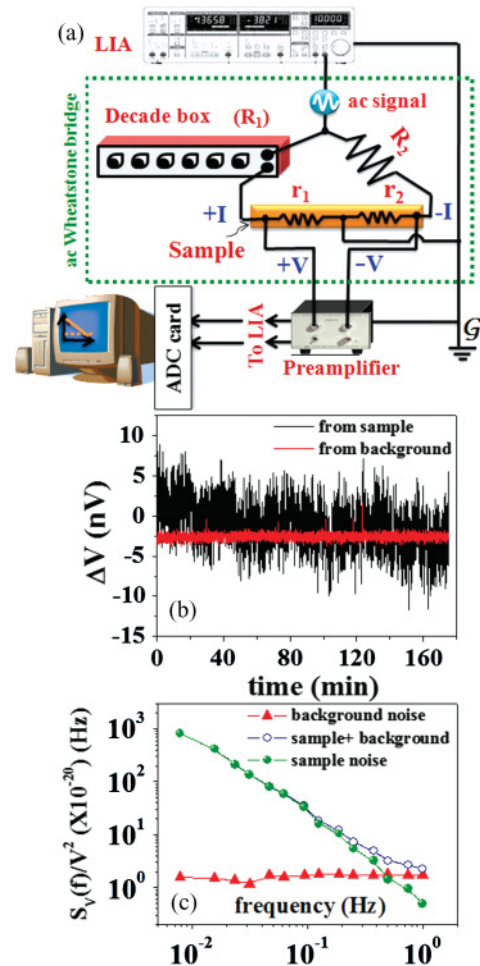


FIG. 1. (Color online) (a) Five-probe noise measurements setup with ac detection scheme. (b) Representative time series data collected simultaneously from the sample (1- $\Omega$  carbon resistor) and the background at  $T = 300 \text{ K}$ . (c) Noise spectral power  $S_V(f)$  along with “white” background noise calculated from the same time series.

signal makes the time series and constitutes the voltage fluctuations  $\Delta V(t)$ . These voltage fluctuations arise from the resistance fluctuation of the current biased sample. The time series was digitized with a 32-bit 200-Ks/s ADC card. A complete set of voltage time series  $[\Delta V(t)]$  consists of  $5 \times 10^6$  data points or even more at each  $T$  (stabilized to within  $\pm 1 \text{ mK}$ ).  $\Delta V(t)$  was processed through a number of digital signal processing (DSP) techniques that include an antialiasing filter, decimation, and digital low-pass filtering.<sup>29</sup> The power spectral density of voltage fluctuations  $S_V(f)$  was obtained numerically by using fast Fourier-transformation (FFT) techniques from the stored and digitally processed time series.<sup>29</sup> The apparatus was calibrated down to a spectral power  $S_V(f) = 10^{-20} \text{ V}^2/\text{Hz}$  by measuring the Nyquist noise  $4k_B T R$  for a calibrated standard resistor at each  $T$ . The noise data for the sample are taken down to  $40 \leq T \leq 300 \text{ K}$ . Below 40 K the resistivity of the material becomes very large for a reliable noise measurement. No heating effects are seen during noise or resistivity measurements.

The investigation of the non-Gaussian component (NGC) was done by two methods that give complementary

information. One method is to plot the probability density function (PDF) from the time series and compare it with a Gaussian probability function by looking for deviation. The PDF [ $P(|\Delta V|)$ ] is obtained as a fluctuation histogram calculated from the time series  $\Delta V(t)$ . Our measurement procedure is sensitive enough for determination of the PDF when the relative variance of fluctuation is less than even a part in  $10^4$ . Data are plotted as  $\ln P(|\Delta V|)$  versus  $(|\Delta V|)^2$ . If there is a measurable NGC in the spectrum it shows up as a deviation from the straight line in the plot.

The development of NGC can also be seen from the normalized second spectrum, which can be estimated from the relation  $S_N^{(2)}(f) = S^{(2)}(f)/[\int_{f_L}^{f_H} S_V(f)/V^2]^2$ .  $S^{(2)}(f) = \int_0^\infty \langle \Delta v^2(t) \Delta v^2(t + \tau) \rangle \cos(2\pi f \tau)$  has been calculated within a chosen  $f$  band ( $f_L = 1$  Hz,  $f_H = 3$  Hz). For a Gaussian fluctuation  $S_N^{(2)}(f)$  is unity and its deviation from unity is a measure of NGC.<sup>30</sup> It is preferable and also advisable to evaluate NGC from the two independent methods mentioned above to avoid any erroneous conclusion from wrong numerical estimation.

### III. RESULTS

In Fig. 2 we plot the  $T$  dependence of the resistivity  $\rho(T)$  for LCMO20. There is a paramagnetic-ferromagnetic transition that occurs at  $T = T_C \simeq 185$  K with a shallow peak in  $\rho(T)$ . (The onset of ferromagnetism has been also established independently through separate magnetic measurements.) The sample shows an activated transport above  $T_C$ . Below  $T_C$ , the temperature dependence is shallow over a limited range followed by an upturn at  $T \simeq 120$  K. The region below  $T_C$  is a region with coexisting phases and is sensitive to the details of sample fabrication.<sup>31</sup> We mark the temperature where the resistivity starts to rise again as the  $T_{\text{FMI}}$ .<sup>6,19,32</sup> The temperature  $T_{\text{FMI}}$  doesn't correspond to a thermodynamic phase transition but the metal-to insulator transition. There exists a mixed phase region with a ferromagnetic metallic (FMM) phase for  $T_{\text{FMI}} < T < T_C$ .<sup>19,20</sup> On cooling down the conduction becomes more dominated by the insulating phase.

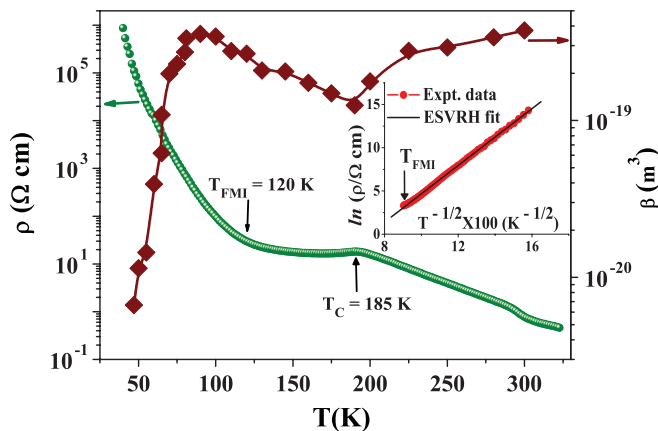


FIG. 2. (Color online) Variation of  $\rho$  (left ordinate) and scaled noise amplitude  $\beta$  (right ordinate) as a function of  $T$  for LCMO20. The  $T_C$  and  $T_{\text{FMI}}$  are marked. Inset shows the  $\ln \rho$  vs  $T^{-1/2}$  plot for  $T \leq T_{\text{FMI}}$ .

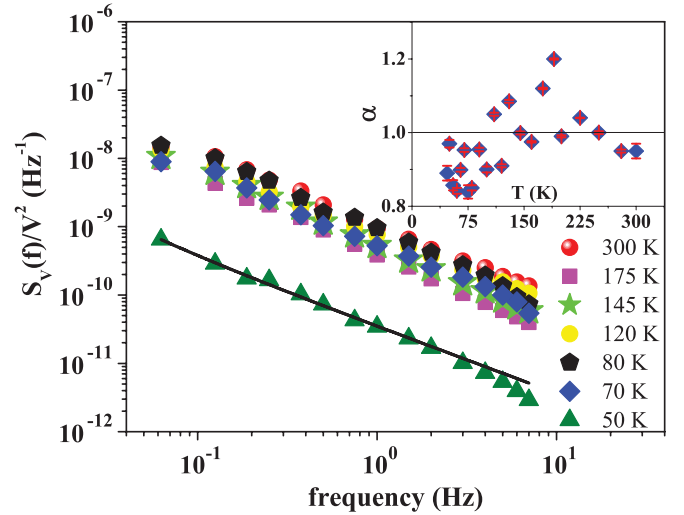


FIG. 3. (Color online) Normalized spectral power  $S_V(f)/V^2$  shown at a few representative temperatures as a function of  $f$ . Inset shows the variation of  $\alpha$  with  $T$ .

The exact value of  $T_{\text{FMI}}$  may depend somewhat on the details of the crystal and the exact condition in which it is grown.

In our samples, at the low  $T$  (below the upturn),  $\rho(T)$  is that of an insulator that follows the Efros-Shklovskii variable range hopping (ESVRH) relation  $\rho = \rho_0 \exp(T_0/T)^{1/2}$  (see the inset of Fig. 2).  $T_0$  is related to the localization length  $\xi = 2.8e^2/(4\pi\epsilon_0\epsilon_1 k_B T_0)$ , where  $\epsilon_1$  is the dielectric constant. The  $T$  dependence of  $\rho(T)$  points toward the existence of a soft gap in the density of states characterized by the Coulomb gap  $\Delta_{\text{CG}}$ .<sup>1</sup> From fitted data we obtain  $\rho_0 = 7.96 \times 10^{-6}$   $\Omega$  cm and  $T_0 = 2.68 \times 10^4$  K. Using  $T_0$ , we obtain a localization length  $\xi \approx 2$   $\text{\AA}$  which is of the order of half the unit cell, indicating strong localization of the polaronic carriers.

In Fig. 2 we also plot the relative variance of the resistance noise,  $\beta = \Omega \langle (\Delta R)^2 \rangle / R^2$ , as a function of  $T$ . The normalized variance  $\langle (\Delta R)^2 \rangle / R^2 \equiv (1/V^2) \int_{f_{\text{min}}}^{f_{\text{max}}} S_V(f) df$  ( $\Omega$  is the experimental volume of the sample). It is noted that the magnitude of  $\beta$  for LCMO20 is much larger (typically by three to four orders) than that observed in single crystals of optimally doped LCMO33 with the FMM state. This difference reflects the basic difference in the ground state of the two systems.

The normalized spectral power  $S_V(f)/V^2$  is shown at a few representative  $T$  as a function of  $f$  in Fig. 3. The spectral power has a  $1/f^\alpha$  dependence with  $\alpha$  very close to 1, although a small but interesting variation in the exponent  $\alpha$  can be seen close to  $T_{\text{FMI}}$  as shown in the inset of Fig. 3. For  $T > T_C$ ,  $\alpha \gtrsim 1$  and  $\alpha < 1$  in the FMI state. This is unlike the observation in doped semiconductors close to the MI boundary<sup>16</sup> where  $\alpha \geq 1$ .

The  $T$  dependence of the spectral power, presented as  $f \cdot S_V(f)/V^2$ , at some representative  $f$  from 0.05 to 10 Hz is shown in Fig. 4. Since  $S_V(f) \sim 1/f$ ,  $f \cdot S_V(f)/V^2$  collapses into almost a single graph for all  $f$  over most of the temperature region. Data presented here are limited for  $T \leq T_C$ , which is the primary focus of this paper. Below  $T_C$ ,  $S_V(f)$  shows a gradual rise until a shallow peak at  $T = T_P$  ( $< T_{\text{FMI}}$ ).  $T_P$  varies approximately from 75 to 90 K depending on

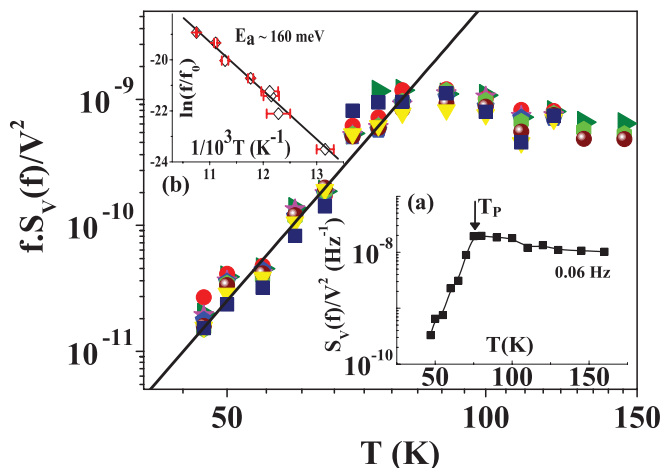


FIG. 4. (Color online)  $f \cdot S_V(f)/V^2$  as a function of  $T$  for a few representative  $f$  from 0.06 to 10 Hz. (a) Variation of  $S_V(f)/V^2$  with  $T$  for  $f = 0.06$  Hz showing a shallow peak at  $T = T_P$  ( $< T_{\text{FMI}}$ ) (see text). (b) Arrhenius plot along with the best fit curve of  $E_a \approx 160$  meV.

the measuring  $f$ .  $T_P$  shifts to a higher value with higher  $f$  following an Arrhenius relation:  $f = f_0 \exp(-E_a/k_B T_P)$  where  $f_0 \sim 10^9$  s<sup>-1</sup>. The inset in Fig. 4 shows the Arrhenius plot which gives the best fit value of  $E_a \approx 160$  meV.

In Fig. 4, below  $T_P$ , the noise power goes down very sharply, with  $T$  following a power-law dependence  $f \cdot S_V(f)/V^2 \propto T^{-\gamma}$ , where  $\gamma$  is  $f$  independent and is  $\approx 8-9$ . The fit to the power law is shown as a solid line. The strong  $T$  dependence of the spectral power in the regime of activated hopping has not been seen before in manganites. Interestingly, such a sharp drop in  $S_V(f)$  at low  $T$  has been seen in some of the doped semiconductors in the hopping regime. In bulk three-dimensional systems, there are only two detailed studies on  $T$  dependence of noise spectral power in the hopping regime.<sup>15,16</sup> Very close to the critical concentration of the MI transition where the carrier concentration  $n/n_c \geq 0.95$ , the magnitude of the noise diverges as  $T$  is reduced.<sup>16</sup> However, somewhat away from the critical region, ( $n/n_c \approx 0.8$ ), the observed behavior is opposite and the spectral power falls as  $T$  decreases. The fall of the spectral power below  $T_{\text{FMI}}$  thus has similarity with that found in doped semiconductors with carrier concentrations  $< 0.85$ .<sup>15</sup>

Equilibrium and nonequilibrium  $1/f$  noise in LCMO ( $x = 0.18$ ) using dc biasing has been reported before.<sup>33</sup> The experiment was done down to 77 K and a nonequilibrium noise was observed at high biasing current. (The smallest  $I$  was 100  $\mu$ A, which is two orders more than the current bias used by us). For  $77 \leq T \leq 300$  K, the paper reported  $S_V/V^2$  is mainly  $T$  independent. While there is a broad qualitative similarity with our data, we find that  $S_V/V^2$  has a shallow temperature dependence which shows distinct features at  $T_C$  and it starts to change significantly at lower  $T$ . In our experiments we could observe the freezing of the fluctuations at lower  $T$ .

In manganites, the electronic states at low  $T$  are expected to be correlated with the development of glassy property. This glassy phase can be due to spin interactions<sup>3,6</sup> according to recent simulation studies<sup>24</sup> with Coulombic origin. Existence of such a correlated state (irrespective of its origin) will lead to NGC in the resistance noise in such systems.<sup>13,15</sup> We have

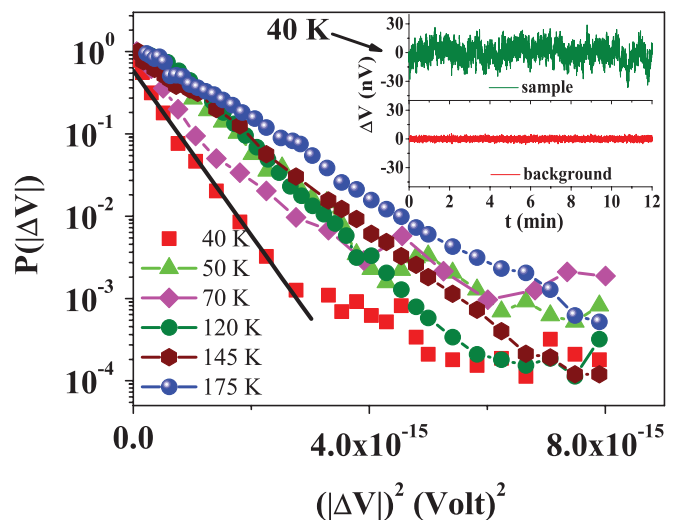


FIG. 5. (Color online) PDF [ $P(|\Delta V|)$ ] as a function of  $(|\Delta V|)^2$  at a few representative  $T$ . Inset shows the time series of the data at 40 K for the sample as well as for the background for comparison. The background, as can be seen, has much less power.

investigated the development of such NGC in the fluctuation using two tests, namely, the direct method of the PDF and also the more sensitive second spectrum method. Figure 5 shows the PDF, plotted as  $\ln P(|\Delta V|)$  versus  $(|\Delta V|)^2$ , for some representative  $T$ . An example of the observed time series is shown in the inset of Fig. 5 at 40 K. In this plot, a straight line will signify a Gaussian PDF. We do not find appreciable deviation (within our detectability) of the PDF from the Gaussian behavior until the temperature is below 100 K. The deviation shows up as a long tail for larger values of  $|\Delta V|$ . The maximum deviation occurs around 70 K, which is the temperature region where the spectral power is also the largest. At lower temperature the spectral power is reduced but the strong deviation from the Gaussian behavior (marked by a line) stays, indicating that the noise has an appreciable NGC in this temperature region where one is in the Coulomb glass phase.

In Fig. 6 we plot  $S_N^{(2)}(f)$  at a few representative  $T$ . The second spectrum has been evaluated at low  $f$ , which is more sensitive to the long-time glassy relaxation, and often correlated fluctuations develop at low  $f$ . The second spectra was found to follow the relation  $S_N^{(2)}(f) \propto f^{-p}$ . The second spectra is flat for ideal Gaussian fluctuations  $p \approx 0$ . The value of  $p$  starts to rise in the temperature range  $T \approx T_C$ , and this may be a signature of the mixed phase due to the presence of an insulating state. The correlation (limited spatial extent) starts building up and starts to contribute to the second spectra. However, for  $T < 100$  K, the exponent  $p$  starts to rise and reaches its highest value at  $T_P$ , where the noise reaches its peak. It then starts to fall down at lower temperatures as the charge fluctuation itself freezes out. We also find a drop in the value of the first spectrum  $S_V(f)$  itself.

We compare the results obtained from the two methods mentioned above. In the direct PDF method we could not detect any deviation from the Gaussian distribution function until the sample is cooled below 100 K, and it persists until  $T = 40$  K although the deviation reaches its maximum around

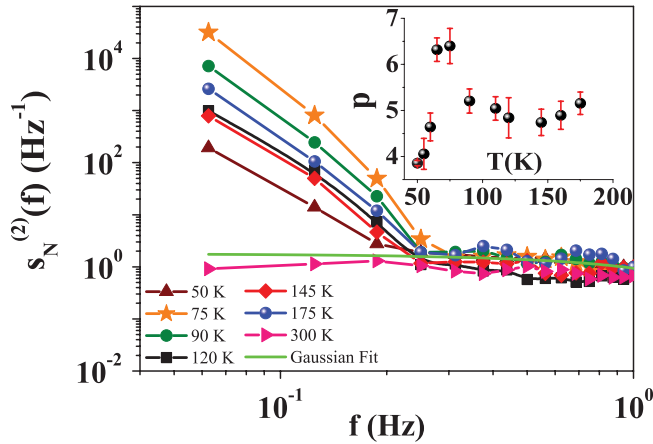


FIG. 6. (Color online) Normalized second spectra for different  $T$ . The calculated Gaussian background is plotted as well.

$T_P$ . Above 100 K, within our detection limit we could not find any deviation from the Gaussian distribution function, while the second spectrum varies as  $f^{-p}$  with the nonzero exponent and is  $\approx 5$  for  $T$  close to  $T_C$  and below. The exponent starts to rise again below 100 K (see the inset of Fig. 6) and reaches a maximum value at  $T \approx T_P$  and falls again as the fluctuation freezes out. From the above two analyses we can infer that the NGC remains at its maximum value (due to the finite value of the  $\Delta_{CG}$ ) until the fluctuation kinetically freezes out below 100 K.

The observed NGC at low  $f$  can be expected if there is a buildup of correlated charge fluctuation with long relaxation times. This can be taken as a signature of entry into a correlated glassy phase.<sup>34</sup> Our experiment shows that in the FMI state (where the resistivity follows ESVRH) the fluctuation can be large until it freezes at a lower temperature ( $< T_P$ ) and the fluctuation has a good non-Gaussian contribution, particularly at low  $f$ . The measuring frequency dependence of  $T_P$  suggests a kinetic freezing of the charge fluctuations.

#### IV. DISCUSSIONS

An important issue which is relevant to the appearance of the electronic glassy phase is the existence of a Coulomb gap ( $\Delta_{CG}$ ) in the charge excitation spectra. Since the glassy phase can set in only at  $T < \Delta_{CG}/k_B$ , it is important that an independent estimate is obtained. For electron glass, this can be obtained from the linear term in specific heat. Specific-heat measurements in these materials at low  $T$  show a linear term indicating a finite density of states  $[N(E_F)]$  at the Fermi level although the states are localized.<sup>22,23</sup> Using  $N(E_F)$  from the experimentally observed linear term, we obtained  $\Delta_{CG} \approx 150$  meV, using the relation<sup>1</sup>  $\Delta_{CG} = e^3 N(E_F)^{1/2} / (4\pi\epsilon_0\epsilon_1)^{3/2}$ . We obtained electronic glassy behavior for the temperatures much smaller than  $\Delta_{CG}/k_B$ , and the proposal for an electronic glassy behavior is justified. Again,  $\Delta_{CG}$  is much larger than that seen in typical semiconductors, which is much smaller than 10 meV<sup>2</sup>. The large  $\Delta_{CG}$  is a direct consequence of large charge-carrier density in these materials, which is much larger than the critical concentration for the MI transition in doped semiconductors. It is also interesting that the activation energy  $E_a$  for the freezing of the charge fluctuation observed

from the noise data is also very close to  $\Delta_{CG}$ , the energy scale that controls activation of charges in the transport process.

We discuss qualitatively the reason for large noise in the FMI state using a recent model,<sup>18,24</sup> which states that there are two types of carriers in manganites, namely, the localized polaronic carriers (referred as  $l$ ) and band-type delocalized carriers (referred as  $b$ ). The simulations based on this model<sup>24</sup> show that the presence of large Coulomb interaction (long range) and disorder (arising from dopant atoms) in doped manganites like LCMO20 can lead to a phase separation in which the conducting  $l$  carrier majority phase is dispersed with islands of nanoscopic puddles of the  $b$  phase. The hopping conduction occurs in the majority phase ( $l$  phase) that percolates through the sample and develops the classical Coulomb glass regime at low  $T$ . For LCMO33, the  $b$  states are occupied and make the majority phase and contribution of  $l$ -type carriers to transport negligible. We propose that while the hopping conduction occurs in the  $l$  phase,  $b$  phases will be thermally occupied and will lead to exchange of carriers between the percolating  $l$  matrix and  $b$  islands, leading to large charge fluctuations. If the size of such a polaronic cluster that makes the main backbone of conduction is  $N_l$  and the variance in fluctuations is  $\langle(\delta N_l)^2\rangle$ , then  $S_V(f)/V^2 = \langle(\delta N_l)^2\rangle/N_l^2$ . Since both the quantities in the numerator and denominator have independent  $T$  dependencies, the resulting  $T$  dependence of  $S_V(f)/V^2$  will be decided by the relative strengths. Generally,  $N_l$  is expected to grow with  $T$  with a power law<sup>34</sup> and to reach a saturation at higher  $T$ .  $\langle(\delta N_l)^2\rangle$  is expected to reflect the charge exchange between the  $b$  and  $l$  regions as well as that between infinite clusters (that is the backbone of conduction) and small clusters within the polaronic glass phase. Below  $T_{FMI}$ , as the nanoscopic inhomogeneity develops and the  $b$  puddles separate out from the  $l$  matrix, the  $b$ - $l$  exchange freezes out. Also the probability of polaronic hopping (that occurs in the Coulomb glass phase of  $l$  carriers) becomes exponentially small at lower  $T$ . These two lead to a rapid drop in  $\langle(\delta N_l)^2\rangle$ . In this temperature range, though,  $N_l$  will also decrease, but the  $\langle(\delta N_l)^2\rangle$  can have a much stronger dependence, leading to a sharp drop of the spectral power. The gradual rise of the noise on cooling below  $T_C$  reflects the growth of  $\langle(\delta N_l)^2\rangle$  because the  $b$  puddles can be occupied and can exchange charges with the  $l$  phase and also  $N_l$  will decrease with  $T$ . The Arrhenius dependence of  $f$  and  $T_P$  also reflects this activated nature of the fluctuation.

The observed large NGC can develop due to two reasons. First, the Coulomb glass phase of polaronic  $l$  carriers can lead to non-Gaussian fluctuations.<sup>34</sup> Second, the nanoscopic phase separation can lead to non-Gaussianity due to the mechanism of random distribution of the current.<sup>35</sup> Both the sources for non-Gaussianity can contribute in tandem due to the nature of the phases present and the transport through them and their relative contributions will also be  $T$  dependent.

It is interesting that the existence of a glassy phase at low temperatures (spin-cluster glass type) has been suggested from NMR relaxation<sup>6</sup> as well as resistance relaxation experiments.<sup>20</sup> For NMR relaxation, the glassy phase begins at  $T \approx 70$  K. From resistance relaxation, the glasslike freezing begins to appear between 75 and 85 K, where spin-glass transition was observed from susceptibility experiments at

$T \approx 67$  K. In our experiment the entry to a electron glasslike freezing of the charge fluctuation occurs at  $T_P$ , which varies approximately from 75 to 90 K depending on the measuring  $f$ . Thus there is a close resemblance to the freezing temperature obtained from different experiments.

The origin of the glassy phase can be long-range Coulomb interactions or interactions in an ensemble of disordered spin or from a pure structural reason with two coexisting different types of orbital orders. Irrespective of the origin, there is indeed a signature of electronic glassy phase and charge fluctuation freezing. It thus appears Coulomb interaction can play an important role in such glassy freezing.

In conclusion, the investigation of noise spectroscopy strongly suggests the existence of the slow correlated motion

of charge carriers in the FMI state. The results establish that the FMI state (where the carriers are predominantly polaronic) is a correlated glassy phase. It has been proposed that the temperature-dependent relative contributions of the two mechanisms like the nanoscopic phase separation and the glassy response in the polaronic-type carriers in LCMO20 can lead to large charge fluctuations leading to large noise with substantial NGC.

#### ACKNOWLEDGMENT

The authors thank the Department of Science and Technology, Government of India for financial support.

\*sudeshna@bose.res.in

†arup@bose.res.in

<sup>1</sup>B. I. Shklovskii and A. L. Efros, *Electronic Properties of Doped Semiconductors* (Springer-Verlag, Berlin, 1984).

<sup>2</sup>A. Amir, Y. Oreg, and Y. Imry, *Annu. Rev. Condens. Matter Phys.* **2**, 235 (2011).

<sup>3</sup>M. Hennion and F. Moussa, *New J. Phys.* **7**, 84 (2005).

<sup>4</sup>C. Zener, *Phys. Rev.* **82**, 403 (1951).

<sup>5</sup>B. B. Van Aken, O. D. Jurchescu, A. Meetsma, Y. Tomioka, Y. Tokura, and T. T. M. Palstra, *Phys. Rev. Lett.* **90**, 066403 (2003).

<sup>6</sup>G. Papavassiliou, M. Pissas, M. Belesi, M. Fardis, J. Dolinsek, C. Dimitropoulos, and J. P. Ansermet, *Phys. Rev. Lett.* **91**, 147205 (2003).

<sup>7</sup>Y. Tokura and N. Nagaosa, *Science* **288**, 462 (2000).

<sup>8</sup>Y. Yamada, O. Hino, S. Nohdo, R. Kanao, T. Inami, and S. Katano, *Phys. Rev. Lett.* **77**, 904 (1996).

<sup>9</sup>A. L. Efros, N. Van Lien, and B. I. Shklovskii, *J. Phys. C* **12**, 1869 (1979).

<sup>10</sup>J. H. Davies, P. A. Lee, and T. M. Rice, *Phys. Rev. Lett.* **49**, 758 (1982); *Phys. Rev. B* **29**, 4260 (1984).

<sup>11</sup>I. Raičević, J. Jaroszyński, D. Popović, C. Panagopoulos, and T. Sasagawa, *Phys. Rev. Lett.* **101**, 177004 (2008).

<sup>12</sup>I. Raičević, D. Popović, C. Panagopoulos, and T. Sasagawa, *Phys. Rev. B* **83**, 195133 (2011).

<sup>13</sup>K. Shtengel and C. C. Yu, *Phys. Rev. B* **67**, 165106 (2003).

<sup>14</sup>A. L. Burin, B. I. Shklovskii, V. I. Kozub, Y. M. Galperin, and V. Vinokur, *Phys. Rev. B* **74**, 075205 (2006).

<sup>15</sup>J. G. Massey and M. Lee, *Phys. Rev. Lett.* **79**, 3986 (1997).

<sup>16</sup>S. Kar, A. K. Raychaudhuri, A. Ghosh, H. v. Löhneysen, and G. Weiss, *Phys. Rev. Lett.* **91**, 216603 (2003).

<sup>17</sup>J. Jaroszyński, D. Popović, and T. M. Klapwijk, *Phys. Rev. Lett.* **89**, 276401 (2002).

<sup>18</sup>T. V. Ramakrishnan, *J. Phys. Condens. Matter* **19**, 125211 (2007).

<sup>19</sup>V. Markovich, I. Fita, R. Puzniak, M. I. Tsindlekht, A. Wisniewski, and G. Gorodetsky, *Phys. Rev. B* **66**, 094409 (2002).

<sup>20</sup>V. Markovich, G. Jung, Y. Yuzhelevski, G. Gorodetsky, A. Szewczyk, M. Gutowska, D. A. Shulyatev, and Ya. M. Mukovskii, *Phys. Rev. B* **70**, 064414 (2004).

<sup>21</sup>V. Markovich, G. Jung, Y. Yuzhelevski, G. Gorodetsky, and Y. M. Mukovskii, *Eur. Phys. J. B* **48**, 41 (2005).

<sup>22</sup>H. Jain, A. K. Raychaudhuri, N. Ghosh, and H. L. Bhat, *Phys. Rev. B* **76**, 104408 (2007).

<sup>23</sup>H. Jain and A. K. Raychaudhuri, *Appl. Phys. Lett.* **93**, 182110 (2008).

<sup>24</sup>V. B. Shenoy, T. Gupta, H. R. Krishnamurthy, and T. V. Ramakrishnan, *Phys. Rev. Lett.* **98**, 097201 (2007).

<sup>25</sup>S. Samanta, A. K. Raychaudhuri, and Joy Mitra, *Phys. Rev. B* **78**, 014427 (2008).

<sup>26</sup>D. A. Shulyatev *et al.*, *J. Cryst. Growth* **198–199**, 511 (1999).

<sup>27</sup>J. H. Scofield, *Rev. Sci. Instrum.* **58**, 985 (1987).

<sup>28</sup>A. K. Raychaudhuri, *Curr. Opin. Solid State Mater. Sci.* **60**, 67 (2002).

<sup>29</sup>A. Ghosh, S. Kar, A. Bid, and A. K. Raychaudhuri, e-print [arXiv:cond-mat/0402130v1](https://arxiv.org/abs/cond-mat/0402130v1) (2004).

<sup>30</sup>G. T. Seidler and S. A. Solin, *Phys. Rev. B* **53**, 9753 (1996).

<sup>31</sup>T. Okuda, Y. Tomioka, A. Asamitsu, and Y. Tokura, *Phys. Rev. B* **61**, 8009 (2000).

<sup>32</sup>V. Markovich, E. Rozenberg, A. I. Shames, G. Gorodetsky, I. Fita, K. Suzuki, R. Puzniak, D. A. Shulyatev, and Ya. M. Mukovskii, *Phys. Rev. B* **65**, 144402 (2002).

<sup>33</sup>X. D. Wu, B. Dolgin, G. Jung, V. Markovich, Y. Yuzhelevski, M. Belogolovskii, and Ya. M. Mukovskii, *Appl. Phys. Lett.* **90**, 242110 (2007).

<sup>34</sup>C. C. Yu, *Phys. Status Solidi C* **1**, 25 (2004).

<sup>35</sup>G. T. Seidler, S. A. Solin, and A. C. Marley, *Phys. Rev. Lett.* **76**, 3049 (1996).